PHYSICAL REVIEW D, VOLUME 70, 096006

Dark matter search after DAMA with ^{73}Ge

V. A. Bednyakov*
Laboratory of Nuclear Problems, Joint Institute for Nuclear Research, 141980 Dubna, Russia

H.V. Klapdor-Kleingrothaus†
Max-Planck-Institut für Kernphysik, Postfach 103980, D-69029, Heidelberg, Germany
(Received 26 April 2004; published 30 November 2004)

The Weakly Interacting Massive Particle (WIMP) is one of the main candidates for the relic dark matter (DM). In the effective low-energy minimal supersymmetric standard model (effMSSM) the neutralino nucleon spin and scalar cross sections in the low-mass regime were calculated. The calculated cross sections are compared with almost all experimental currently available exclusion curves for spin-dependent WIMP-proton and WIMP-neutron cross sections. It is demonstrated that *in general* about 2 orders of magnitude improvement of the current DM experiment sensitivities is needed to reach the (effMSSM) supersymmetric (SUSY) predictions. At the current level of accuracy it looks reasonable to safely neglect *subdominant spin WIMP nucleon contributions* analyzing the data from spin-nonzero targets. To avoid misleading discrepancies between data and SUSY calculations it is, however, preferable to use a mixed spin-scalar coupling approach. This approach is applied to estimate future prospects of experiments with the odd-neutron high-spin isotope ^{73}Ge. It is noticed that the DAMA evidence favors the light Higgs sector in the effMSSM, a high event rate in a ^{73}Ge detector and relatively high up-going muon fluxes from relic neutralino annihilations in the Earth and the Sun.

DOI: 10.1103/PhysRevD.70.096006 PACS numbers: 11.30.Pb, 12.60.Jv, 95.35.+d

I. INTRODUCTION

Nowadays the main efforts and expectations in the direct dark matter searches are concentrated in the field of so-called spin-independent (or scalar) interaction of a dark matter Weakly Interacting Massive Particle (WIMP) with a target nucleus. The lightest supersymmetric (SUSY) particle (LSP) neutralino is assumed to be the best WIMP dark matter (DM) candidate. It is believed that for heavy enough nuclei this spin-independent (SI) interaction of DM particles with nuclei usually gives the dominant contribution to the expected event rate of its detection. The reason is the strong (proportional to the squared mass of the target nucleus) enhancement of SI WIMP-nucleus interaction. The results currently obtained in the field are usually presented in the form of exclusion curves due to nonobservation of the WIMPs. For a fixed mass of the WIMP the cross sections of SI elastic WIMP-nucleon interaction located above these curves are excluded.

Only the DAMA collaboration claims observation of first evidence for the dark matter signal, due to registration of the annual modulation effect [1–3]. The DAMA results are shown in the middle of Fig. 1 as two contours together with some set of other exclusion curves already obtained (solid lines) and expected in the future (dashed lines). Aimed since more than one decade at the DM particle direct detection, the DAMA experiment (DAMA/NaI) with 100 kg of highly radio-pure NaI (Tl) scintillator detectors successfully operated until July 2002 at the Gran Sasso National Laboratory of the Instituto Nazionale di Fisica Nucleare (I.N.F.N.). On the basis of the results obtained over seven annual cycles (107 731 kg/day total exposure) the presence of a WIMP model-independent annual modulation signature was demonstrated and the WIMP presence in the galactic halo is strongly supported at 6.3 σ C.L. [2]. The main result of the DAMA observation of the annual modulation signature is the low-mass region of the WIMPs ($40 < m_\chi < 150$ GeV), provided these WIMPs are cold dark matter particles. Although there are beautiful other experiments like EDELWEISS, CDMS, etc., which give sensitive exclusion curves, no one of them at present has the sensitivity to look for the modulation effect. Because of the small target masses and short running times the CDMS and EDELWEISS are unable to see positive annual modulation signature of the WIMP interactions. Often the results of these and DAMA experiments have been compared not on the basis of complete analysis including simultaneously SI and spin-dependent (SD) WIMP-nucleus interaction. This sometimes gives rise to quite some confusion in literature. There are also other attempts to reconcile the DAMA conflict with the other experiments [4–7].

It is obvious that such a serious claim should be verified at least by one other completely independent experiment. To confirm this DAMA result one should perform a new experiment which would have (in reasonable time) the same or better sensitivity to the annual modulation signal (and also it would be better to locate this new setup in another low-background underground laboratory). This

*Email: Vadim.Bednyakov@jinr.ru
†Email: H.Klapdor@mpi-hd.mpg.de

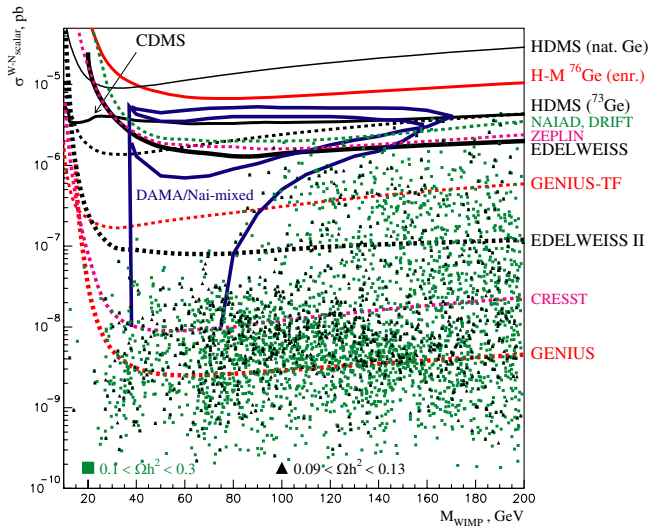

FIG. 1 (color online). WIMP-nucleon cross section limits in pb for scalar (spin-independent) interactions as a function of the WIMP-mass in GeV. Shown are contour lines for some of the present experimental limits (solid lines) and some of projected experiments (dashed lines). The closed DAMA/NaI contour corresponds to a complete neglection of spin-dependent WIMP-nucleon interaction ($\sigma_{SD} = 0$), while the open contour is obtained with the assumption that $\sigma_{SD} = 0.08$ pb [2]. Our theoretical expectations are shown by scatter plots for a relic neutralino density $0.1 < \Omega_\chi h_0^2 < 0.3$ (green boxes) and to WMAP relic density $0.094 < \Omega_\chi h_0^2 < 0.129$ (black triangles). Similar estimations one can find, for example, in [12,53,54].

mission, in particular, could be executed by new generation experiments with large enough mass of germanium high-purity (HP) detectors both with spin (^{73}Ge) and spinless (natural Ge). Because of kinematic reasons ($M_{\text{Target}} \approx M_{\text{WIMP}}$) these germanium isotopes with their masses being almost equal to the mass of the DAMA WIMP (about 70 GeV) have the best efficiency for such WIMP detection. A new setup with "naked" Ge detectors in liquid nitrogen (GENIUS-TF) is already installed and works over months under the low-background conditions of the Gran Sasso Laboratory [8]. The GENIUS-TF experiment is planned to be sensitive to the annual modulation signal with data taking over about five years with a large enough mass of the Ge detectors [9].

In this paper we start from the final results of the DAMA collaboration based on the seven-year long measurements of the annual modulation [2] and consider their possible consequences for dark matter search with high-spin ^{73}Ge detectors like Heidelberg Dark Matter Search (HDMS) [10]. We also briefly consider some aspects of the spin-dependent (or axial-vector) interaction of the DM WIMPs with nuclei. There are at least three reasons to think that this SD interaction could be very important. First, contrary to the only one constraint for SUSY models available from the scalar WIMP-nucleus interaction, the spin WIMP-nucleus interaction supplies us with two such constraints (see for example [11] and formulas below). Second, one can notice [12,13] that even with a very sensitive DM detector (say, with a sensitivity of 10^{-5}events/day/kg) which is sensitive only to the WIMP-nucleus scalar interaction (with spinless target nuclei) one can, in principle, miss a DM signal. To safely avoid such a situation one should have a spin-sensitive DM detector, i.e., a detector with spin-nonzero target nuclei. Finally, there is a complicated nuclear spin structure, which, for example, possesses the so-called long q-tail form-factor behavior. Therefore for heavy mass target nuclei and heavy WIMP masses the SD efficiency to detect a DM signal is much higher than the SI efficiency [14].

II. APPROACH TO OUR CALCULATIONS

A. Cross sections and event rate

A dark matter event is elastic scattering of a relic neutralino χ from a target nucleus A producing a nuclear recoil E_R which can be detected by a suitable detector. The differential event rate in respect to the recoil energy is the subject of experimental measurements. The rate depends on the distribution of the relic neutralinos in the solar vicinity $f(v)$ and the cross section of neutralino nucleus elastic scattering [2,15–22]. The differential event rate per unit mass of the target material has the form

$$\frac{dR}{dE_R} = N_T \frac{\rho_\chi}{m_\chi} \int_{v_{\min}}^{v_{\max}} dv f(v) v \frac{d\sigma}{dq^2}(v, q^2). \tag{1}$$

The nuclear recoil energy $E_R = q^2/(2M_A)$ is typically about $10^{-6} m_\chi$ and $N_T = \mathcal{N}/A$ is the number density of target nuclei, where $\mathcal{N}$ is the Avogadro number and A is the atomic mass of the nuclei with mass M_A. The neutralino nucleus elastic scattering cross section for spin-nonzero ($J \neq 0$) nuclei contains SI and SD terms [14,23,24]:

$$\begin{aligned}\frac{d\sigma^A}{dq^2}(v, q^2) &= \frac{\sum |\mathcal{M}|^2}{\pi v^2 (2J+1)} \\ &= \frac{S^A_{\text{SD}}(q^2)}{v^2(2J+1)} + \frac{S^A_{\text{SI}}(q^2)}{v^2(2J+1)} \\ &= \frac{\sigma^A_{\text{SD}}(0)}{4\mu_A^2 v^2} F^2_{\text{SD}}(q^2) + \frac{\sigma^A_{\text{SI}}(0)}{4\mu_A^2 v^2} F^2_{\text{SI}}(q^2).\end{aligned} \tag{2}$$

The normalized $[F^2_{\text{SD,SI}}(0) = 1]$ nonzero-momentum transfer nuclear form factors

$$F^2_{\text{SD,SI}}(q^2) = \frac{S^A_{\text{SD,SI}}(q^2)}{S^A_{\text{SD,SI}}(0)}, \tag{3}$$

are defined via nuclear structure functions [14,23,24]

$$S^A_{\rm SI}(q) = \sum_{L{\rm even}} |\langle J||C_L(q)||J\rangle|^2 \simeq |\langle J||C_0(q)||J\rangle|^2, \quad (4)$$

$$S^A_{\rm SD}(q) = \sum_{L{\rm odd}}\Big[|\langle N||\mathcal{T}^{el5}_L(q)||N\rangle|^2 + |\langle N||\mathcal{L}^5_L(q)||N\rangle|^2 \Big]. \quad (5)$$

The transverse electric $\mathcal{T}^{el5}(q)$ and longitudinal $\mathcal{L}^5(q)$ multipole projections of the axial-vector current operator, and the scalar function $C_L(q)$ are given in the form

$$\mathcal{T}^{el5}_L(q) = \frac{1}{\sqrt{2L+1}}\sum_i \frac{a_0 + a_1\tau^i_3}{2} \times\Big[-\sqrt{L}M_{L,L+1}(q\vec{r}_i) + \sqrt{L+1}M_{L,L-1}(q\vec{r}_i)\Big],$$

$$\mathcal{L}^5_L(q) = \frac{1}{\sqrt{2L+1}}\sum_i\Big[\frac{a_0}{2} + \frac{a_1 m^2_\pi \tau^i_3}{2(q^2+m^2_\pi)}\Big] \times\Big[\sqrt{L+1}M_{L,L+1}(q\vec{r}_i) + \sqrt{L}M_{L,L-1}(q\vec{r}_i)\Big],$$

$$C_L(q) = \sum_{i,\ \text{nucleons}} c_0 j_L(qr_i)Y_L(\hat{r}_i),$$

$$C_0(q) = \sum_i c_0 j_0(qr_i)Y_0(\hat{r}_i),$$

where $a_{0,1} = a_n \pm a_p$ and $M_{L,L'}(q\vec{r}_i) = j_{L'}(qr_i)\times[Y_{L'}(\hat{r}_i)\vec{\sigma}_i]^L$ [14,23,24]. The nuclear SD and SI cross sections at $q=0$ in (2) can be presented as follows

$$\sigma^A_{\rm SI}(0) = \frac{4\mu^2_A S_{\rm SI}(0)}{(2J+1)} = \frac{\mu^2_A}{\mu^2_p}A^2\sigma^p_{\rm SI}(0), \quad (6)$$

$$\sigma^A_{\rm SD}(0) = \frac{4\mu^2_A S_{\rm SD}(0)}{(2J+1)} = \frac{4\mu^2_A}{\pi}\frac{(J+1)}{J}\{a_p\langle \mathbf{S}^A_p\rangle + a_n\langle \mathbf{S}^A_n\rangle\}^2 \quad (7)$$

$$= \frac{\mu^2_A}{\mu^2_p}\frac{(J+1)}{3J}\Big\{\sqrt{\sigma^p_{\rm SD}(0)}\langle \mathbf{S}^A_p\rangle + {\rm sign}(a_p a_n)\sqrt{\sigma^n_{\rm SD}(0)}\langle \mathbf{S}^A_n\rangle\Big\}^2 \quad (8)$$

$$= \frac{\mu^2_A}{\mu^2_p}\frac{4}{3}\frac{J+1}{J}\sigma^{pn}_{\rm SD}(0)\Big\{\langle \mathbf{S}^A_p\rangle\cos\theta + \langle \mathbf{S}^A_n\rangle\sin\theta\Big\}^2. \quad (9)$$

Here $\mu_A = \frac{m_\chi M_A}{m_\chi + M_A}$ is the reduced χ-A mass, and $\mu_p = \mu_n$ is assumed. Following Bernabei *et al.* [2,25] the effective spin WIMP-nucleon cross section $\sigma^{pn}_{\rm SD}(0)$ and the coupling mixing angle θ were introduced

$$\sigma^{pn}_{\rm SD}(0) = \frac{\mu^2_p}{\pi}\frac{4}{3}\Big[a^2_p + a^2_n\Big], \qquad \tan\theta = \frac{a_n}{a_p}; \quad (10)$$

$$\sigma^p_{\rm SD} = \sigma^{pn}_{\rm SD}\times\cos^2\theta, \quad \sigma^n_{\rm SD} = \sigma^{pn}_{\rm SD}\times\sin^2\theta. \quad (11)$$

The zero-momentum transfer proton and neutron SI and SD cross sections

$$\sigma^p_{\rm SI}(0) = 4\frac{\mu^2_p}{\pi}c^2_0, \qquad c_0 \equiv c^{(p,n)}_0 = \sum_q C_q f^{(p,n)}_q; \quad (12)$$

$$\sigma^{p,n}_{\rm SD}(0) = 12\frac{\mu^2_{p,n}}{\pi}a^2_{p,n}, \qquad a_p = \sum_q \mathcal{A}_q\Delta^{(p)}_q, \quad a_n = \sum_q \mathcal{A}_q\Delta^{(n)}_q, \quad (13)$$

depend on the effective neutralino-quark scalar C_q and axial-vector $\mathcal{A}_q$ couplings from the effective Lagrangian

$$\mathcal{L}_{\rm eff} = \sum_q(\mathcal{A}_q\times\bar{\chi}\gamma_\mu\gamma_5\chi\times\bar{q}\gamma^\mu\gamma_5 q + C_q\times\bar{\chi}\chi\times\bar{q}q) + \ldots, \quad (14)$$

and on the spin ($\Delta^{(p,n)}_q$) and mass ($f^{(p,n)}_q$) structure of nucleons. The parameters $a_{p(n)}$ in (13) can be considered as effective WIMP-proton (neutron) couplings. The factors $\Delta^{(p,n)}_q$ in (13) parameterize the quark spin content of the nucleon and are defined by the relation $2\Delta^{(n,p)}_q s^\mu \equiv \langle p,s|\bar{\psi}_q\gamma^\mu\gamma_5\psi_q|p,s\rangle_{(p,n)}$. A global QCD analysis for the g_1 structure functions [26] including $\mathcal{O}(\alpha^3_s)$ corrections supplied us with the values [27]

$$\Delta^{(p)}_u = \Delta^{(n)}_d = 0.78\pm0.02, \quad \Delta^{(p)}_d = \Delta^{(n)}_u = -0.48\pm0.02, \quad \Delta^{(p)}_s = \Delta^{(n)}_s = -0.15\pm0.02. \quad (15)$$

The nuclear spin (proton, neutron) operator is defined as follows

$$\mathbf{S}_{p,n} = \sum_i^A \mathbf{s}_{p,n}(i), \quad (16)$$

where i runs over all nucleons. Further the convention is used that all angular momentum operators are evaluated in their z-projection in the maximal M_J state, e.g.,

$$\langle \mathbf{S}\rangle \equiv \langle N|\mathbf{S}|N\rangle \equiv \langle J, M_J = J|S_z|J, M_J = J\rangle. \quad (17)$$

Therefore $\langle \mathbf{S}_{p(n)}\rangle$ is the spin of the proton (neutron) averaged over all nucleons in the nucleus A. The cross sections at zero-momentum transfer show strong dependence on the nuclear structure of the ground state [28–30].

The relic neutralinos in the halo of our Galaxy have a mean velocity of $\langle v\rangle \simeq 300$ km/s $= 10^{-3}c$. When the product $q_{\rm max}R \ll 1$, where R is the nuclear radius and $q_{\rm max} = 2\mu_A v$ is the maximum momentum transfer in the χ-A scattering, the matrix element for the SD χ-A scattering reduces to a very simple form (*zero-momentum transfer limit*) [28,29]:

$$\mathcal{M} = C\langle N|a_p\mathbf{S}_p + a_n\mathbf{S}_n|N\rangle \times \mathbf{s}_\chi = C\Lambda\langle N|\mathbf{J}|N\rangle \times \mathbf{s}_\chi. \tag{18}$$

Here $\mathbf{s}_\chi$ is the spin of the neutralino, and

$$\Lambda = \frac{\langle N|a_p\mathbf{S}_p + a_n\mathbf{S}_n|N\rangle}{\langle N|\mathbf{J}|N\rangle} = \frac{\langle N|(a_p\mathbf{S}_p + a_n\mathbf{S}_n) \times \mathbf{J}|N\rangle}{J(J+1)}. \tag{19}$$

It is seen that the χ couples to the spin carried by the protons and the neutrons. The normalization C involves the coupling constants, masses of the exchanged bosons and various LSP mixing parameters that have no effect upon the nuclear matrix element [31]. In the $q = 0$ limit the spin structure function (5) reduces to

$$S^A_{\rm SD}(0) = \frac{2J+1}{\pi}\Lambda^2 J(J+1). \tag{20}$$

The first model to estimate the spin content in the nucleus for the dark matter search was the independent single-particle shell model (ISPSM) used originally by Goodman and Witten [32] and later in [17,33,34]. Here the ground state value of the nuclear total spin J can be described by that of one extra nucleon interacting with the effective potential of the nuclear core. There are nuclear structure calculations (including nonzero-momentum approximation) for spin-dependent neutralino interaction with helium ^{3}He [35]; fluorine ^{19}F [30,35,36]; sodium ^{23}Na [29,30,35,36]; aluminum ^{27}Al [28]; silicon ^{29}Si [24,30,36]; chlorine ^{35}Cl [24]; potassium ^{39}K [28]; germanium ^{73}Ge [24,37]; niobium ^{93}Nd [38]; iodine ^{127}I [29]; xenon ^{129}Xe [29] and ^{131}Xe [14,29,39]; tellurium ^{123}Te [39] and ^{125}Te [29]; lead ^{208}Pb [35,40]. The zero-momentum case is also investigated for Cd, Cs, Ba, and La in [39,41,42].

There are several approaches to more accurate calculations of the nuclear structure effects relevant to the dark matter detection. The list of the models includes the Odd-Group Model (OGM) of Engel and Vogel [43] and their extended OGM (EOGM) [23,43]; Interacting Boson Fermion Model (IBFM) of Iachello, Krauss, and Maino [42]; Theory of Finite Fermi Systems (TFFS) of Nikolaev and Klapdor-Kleingrothaus [44]; Quasi Tamm-Dancoff Approximation (QTDA) of Engel [14]; different shell model treatments (SM) by Pacheco and Strottman [41]; by Engel, Pittel, Ormand, and Vogel [38] and Engel, Ressell, Towner, and Ormand, [28], by Ressell *et al.* [24] and Ressell and Dean [29]; by Kosmas, Vergados *et al.* [30,35,40]; the so-called ''hybrid'' model of Dimitrov, Engel, and Pittel [37] and perturbation theory based on calculations of Engel *et al.* [28].

The direct detection rate (1) in a nucleus A integrated over the recoil energy interval from threshold energy ϵ until maximal energy ε is a sum of SD and SI contributions:

$$R(\epsilon,\varepsilon) = \alpha(\epsilon,\varepsilon,m_\chi)\sigma^p_{\rm SI} + \beta(\epsilon,\varepsilon,m_\chi)\sigma^{pn}_{\rm SD}; \tag{21}$$

$$\begin{aligned}
\alpha(\epsilon,\varepsilon,m_\chi) &= N_T\frac{\rho_\chi M_A}{2m_\chi\mu_p^2}A^2A_{\rm SI}(\epsilon,\varepsilon),\\
\beta(\epsilon,\varepsilon,m_\chi) &= N_T\frac{\rho_\chi M_A}{2m_\chi\mu_p^2}\frac{4}{3}\frac{J+1}{J}\Big(\langle\mathbf{S}^A_p\rangle\cos\theta\\
&\quad + \langle\mathbf{S}^A_n\rangle\sin\theta\Big)^2 A_{\rm SD}(\epsilon,\varepsilon);\\
A_{\rm SI,SD}(\epsilon,\varepsilon) &= \frac{\langle v\rangle}{\langle v^2\rangle}\int_\epsilon^\varepsilon dE_{\rm R}F^2_{\rm SI,SD}(E_{\rm R})I(E_{\rm R}).
\end{aligned} \tag{22}$$

To estimate the event rate (21) one needs to know a number of quite uncertain astrophysical and nuclear structure parameters as well as the precise characteristics of the experimental setup (see, for example, the discussions in [2,45]).

B. Effective low-energy MSSM

To obtain as much as general predictions it appeared more convenient to work within a phenomenological SUSY model whose parameters are defined directly at the electroweak scale, relaxing completely constraints following from any unification assumption as, for example, in [46–51], and which is called an effective scheme of MSSM (effMSSM) in [52], and later by some people low-energy effective supersymmetric theory (LEEST) in [53,54]. In our previous calculations in effMSSM [12,13,20–22,46,55–58] we have adopted some effective scheme (with nonuniversal scalar masses and with nonuniversal gaugino soft masses) which lead to large values for direct detection rates of DM neutralinos.

Our MSSM parameter space is determined by the entries of the mass matrices of neutralinos, charginos, Higgs bosons, sleptons and squarks. The relevant definitions one can find in [46]. The list of free parameters includes: $\tan\beta$ is the ratio of neutral Higgs boson vacuum expectation values, μ is the bilinear Higgs parameter of the superpotential, $M_{1,2}$ are soft gaugino masses, M_A is the CP-odd Higgs mass, $m^2_{\tilde{Q}}$, $m^2_{\tilde{U}}$, $m^2_{\tilde{D}}$ ($m^2_{\tilde{L}}$, $m^2_{\tilde{E}}$) are squared squark (slepton) mass parameters for the first and second generation, $m^2_{\tilde{Q}_3}$, $m^2_{\tilde{T}}$, $m^2_{\tilde{B}}$ ($m^2_{\tilde{L}_3}$, $m^2_{\tilde{\tau}}$) are squared squark (slepton) mass parameters for third generation and A_t, A_b, A_τ are soft trilinear couplings for the third generation. The third gaugino mass parameter M_3 defines the mass of the gluino in the model and is determined by means of the Grand Unification Theory (GUT) assumption $M_2 = 0.3M_3$.

Contrary to our previous considerations [12,13,20–22,46,55–58] and aiming at exploration of the MSSM parameter space in the DAMA-inspired domain of the lower masses of the LSP ($m_\chi < 200$ GeV), we narrowed in the present work the intervals of the randomly scanned

parameter space to the following:

$$-200\ \text{GeV} < M_1 < 200\ \text{GeV},$$

$$-1\ \text{TeV} < M_2, \mu < 1\ \text{TeV},$$

$$-2\ \text{TeV} < A_t < 2\ \text{TeV}, \qquad 10 < \tan\beta < 50, \qquad (23)$$

$$50\ \text{GeV} < M_A < 500\ \text{GeV},$$

$$10\ \text{GeV}^2 < m^2_{\tilde{Q},\tilde{Q}_3}, m^2_{\tilde{L},\tilde{L}_3} < 10^6\ \text{GeV}^2.$$

As previously, we assume that squark masses are basically degenerate. Bounds on flavor-changing neutral currents imply that squarks with equal gauge quantum numbers must be close in mass [59–61]. With the possible exception of third generation squarks the assumed degeneracy holds almost model-independently [59]. Therefore for other sfermion mass parameters as before in [12,13,46,55–58] we used the relations $m^2_{\tilde{U}} = m^2_{\tilde{D}} = m^2_{\tilde{Q}}$, $m^2_{\tilde{E}} = m^2_{\tilde{L}}$, $m^2_{\tilde{T}} = m^2_{\tilde{B}} = m^2_{\tilde{Q}_3}$, $m^2_{\tilde{E}_3} = m^2_{\tilde{L}_3}$. The parameters A_b and A_τ are fixed to be zero.

We have included the current experimental upper limits on sparticle and Higgs masses from the Particle Data Group [62]. For example, we use as previously the following lower bounds for the SUSY particles: $M_{\tilde{\chi}^\pm_{1,2}} \geq 100$ GeV for charginos, $M_{\tilde{\chi}^0_{1,2,3}} \geq 45, 76, 127$ GeV for non-LSP neutralinos, respectively; $M_{\tilde{\nu}} \geq 43$ GeV for sneutrinos, $M_{\tilde{e}_R} \geq 70$ GeV for selectrons, $M_{\tilde{q}} \geq 210$ GeV for squarks, $M_{\tilde{t}_1} \geq 85$ GeV for light top-squark, $M_{H^0} \geq 100$ GeV for neutral Higgs bosons, $M_{\text{H}^+} \geq 70$ GeV for the charged Higgs boson. Also the limits on the rare $b \to s\gamma$ decay [63,64] following [65–68] have been imposed.

For each point in the MSSM parameter space (MSSM model) we have evaluated the relic density of the light neutralinos $\Omega_\chi h^2_0$ with our code [56–58] based on [69], taking into account all coannihilation channels with two-body final states that can occur between neutralinos, charginos, sleptons, stops, and sbottoms, as long as their masses are $m_i < 2m_\chi$. We assume as before $0.1 < \Omega_\chi h^2 < 0.3$ for the cosmologically interesting region and we also consider the WMAP reduction of the region to $0.094 < \Omega_\chi h^2 < 0.129$ [70,71] and a possibility of the LSP to be not a unique DM candidate with much smaller relic density $0.002 < \Omega h^2 < 0.1$.

III. RESULTS AND DISCUSSIONS

A. Cross sections in the effMSSM for $m_\chi < 200$ GeV

The results of our evaluations of the zero-momentum transfer proton and neutron SI (12) and SD (13) cross sections in the effMSSM approach within the DAMA-inspired parameter space of (23) are shown as scatter plots in Figs. 2–4.

Scatter plots with individual cross sections of SD and SI interactions of WIMPs with proton and neutron are given in Fig. 2 as functions of the LSP mass. In the figure filled circles correspond to cross sections calculated when the neutralino relic density should just not overclose the Universe ($0.0 < \Omega_\chi h^2_0 < 1.0$). Filled squares show the same cross sections when one assumes the relic neutralinos to be not the only DM particles and give only subdominant contribution to the relic density $0.002 < \Omega_\chi h^2_0 < 0.1$. In the left panel of Fig. 2 these cross sections are shown with the triangles corresponding to the case when the relic neutralino density is in the bounds previously associated with a so-called flat and accelerating Universe $0.1 < \Omega_\chi h^2_0 < 0.3$. The triangles in the right panel in Fig. 2 correspond to imposing the new WMAP [70,71] constraint on matter relic density $0.094 < \Omega_\chi h^2_0 < 0.129$. Despite a visible reduction of the allowed domain for the relic density due to the WMAP result the upper bounds for the spin-dependent and the spin-independent WIMP-nucleon cross section are not significantly affected. From the comparison of circle and square distributions, as expected, follows that the largest cross section values correspond to smallest values of the Ω_χ, especially for smaller LSP masses. It is seen that the LSP as a subdominant DM particle favors the large SD and SI

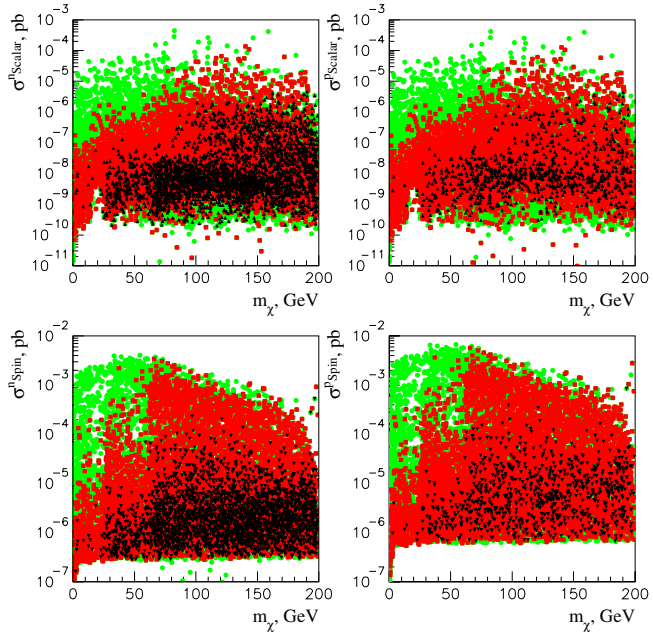

FIG. 2 (color online). Cross sections of the spin-dependent (spin) and the spin-independent (scalar) interactions of WIMPs with the proton and the neutron. Filled circles correspond to the relic neutralino density $0 < \Omega_\chi h^2_0 < 1$, squares correspond to the subdominant relic neutralino contribution $0.002 < \Omega_\chi h^2_0 < 0.1$, and triangles correspond to the relic neutralino density $0.1 < \Omega_\chi h^2_0 < 0.3$ (left panel) and to the WMAP relic density $0.094 < \Omega_\chi h^2_0 < 0.129$ (right panels).

cross sections. Furthermore the maximal SD and SI cross sections in Fig. 2 (circles) come from very small relic density values $0.0 < \Omega_\chi h_0^2 < 0.002$.

One can see also that in our effMSSM with parameters from (23) the lower bound value in the relic density constraints (as, for example, 0.094 in the case of WMAP) restricts from below the allowed masses of the LSP in accordance with previous considerations [20,72].

The spin-dependent and spin-independent WIMP-proton cross sections as functions of input MSSM parameters μ, M_A, $\tan\beta$, and $m^2_{\tilde{Q}}$ are shown in Figs. 3 and 4. There is no noticeable dependence of these scatter plots on the other free parameters from our set (23). From these figures one can see the similarity of the scatter plots for spin-dependent and scalar cross sections as functions of μ and $m^2_{\tilde{Q}}$. Decreases of both lower bounds of the cross sections with $m^2_{\tilde{Q}}$ occur due to increases of masses of squarks, which enter the s-channel intermediate states. Both spin-dependent and spin-independent cross sections increase when $|\mu|$ decreases, in agreement with literature [47,73,74] and our previous calculations [12,46]. The increase of the scalar cross sections generally is connected with an increase of the Higgsino admixture of the LSP and increase of Higgsino-gaugino interference which enters this cross section [73–75]. The reason of the Higgsino growth can be nonuniversality of scalar soft masses [74], variation of intermediate unification scale [75], or focus point regime of the supersymmetry [73]. There is no visible sensitivity of the SD cross sections to $\tan\beta$ and M_A (Higgs bosons do not contribute) but the SI cross section possesses remarkable dependence on these parameters. The SI cross sections rather quickly drop with growth of the CP-odd Higgs mass M_A and increase with $\tan\beta$ [22,46,52,74–77]. The different $\tan\beta$- and M_A-dependence of the SD and SI cross section as well as the general about 2 order of magnitude excess of the spin-dependent cross sections over spin-independent cross sections may be important for observations [12,13,55,78,79]. It is interesting to note that maximal values for the LSP-proton SD cross section can be obtained in the pure Higgsino case (when only Z-exchange contributes) at a level of 5×10^{-2} pb. This value is almost reached by points from our scatter plots in Figs. 2 and 4.

B. Constraints on WIMP-nucleon spin interactions

For the spin-zero nuclear target the experimentally measured event rate (1) of direct DM particle detection, via formula (2) is connected with the zero-momentum WIMP-proton (neutron) cross section (6). The zero-momentum scalar WIMP-proton (neutron) cross section $\sigma^p_{\rm SI}(0)$ can be expressed through effective neutralino-quark couplings C_q (14) by means of expression (12). These couplings C_q (as well as $\mathcal{A}_q$) can be directly connected with the fundamental parameters of a SUSY model such as $\tan\beta$, $M_{1,2}$, μ, masses of sfermions and Higgs bosons, etc. Therefore experimental limitations on

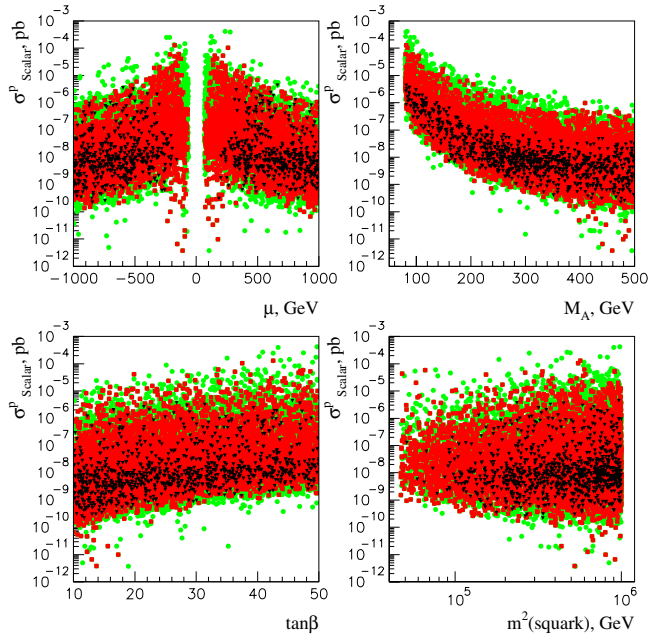

FIG. 3 (color online). Cross sections of WIMP-proton spin-independent interactions as function of input parameters μ, M_A, $\tan\beta$, and $m^2_{\tilde{Q}}$ with the same notations as in Fig. 2 for used constraints on the neutralino relic density $\Omega_\chi h^2$.

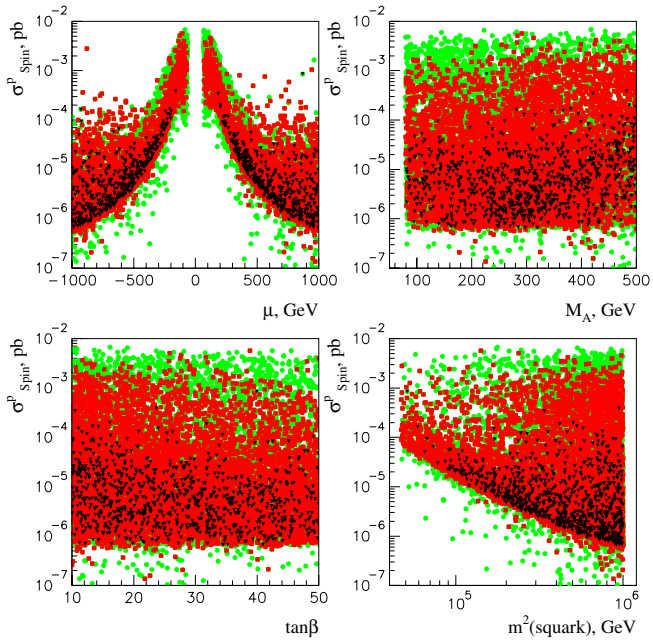

FIG. 4 (color online). Cross sections of WIMP-proton spin-dependent interactions as function of input parameters μ, M_A, $\tan\beta$, and $m^2_{\tilde{Q}}$ with the same notations as in Fig. 2 for used constraints on the neutralino relic density $\Omega_\chi h^2$.

the spin-independent neutralino-nucleon cross section supply us with a constraint on the fundamental parameters of an underlying SUSY model.

In the case of the spin-dependent WIMP-nucleus interaction from a measured differential rate (1) one first extracts a limitation for $\sigma^A_{\rm SD}(0)$, and therefore has in principle two constraints [11] for the neutralino-proton a_p and neutralino-neutron a_n effective spin couplings, as follows from relation (7). From (7) one can also see that contrary to the spin-independent case (6) there is no, in general, factorization of the nuclear structure for $\sigma^A_{\rm SD}(0)$. Both proton $\langle \mathbf{S}^A_p \rangle$ and neutron $\langle \mathbf{S}^A_n \rangle$ spin contributions simultaneously enter into formula (7) for the SD WIMP-nucleus cross section $\sigma^A_{\rm SD}(0)$.

In the earlier considerations based on the OGM [23,43] one assumed that the nuclear spin is carried by the ''odd'' unpaired group of protons or neutrons and only one of either $\langle \mathbf{S}^A_n \rangle$ or $\langle \mathbf{S}^A_p \rangle$ is nonzero (the same is true in the ISPSM [17,32–34]). In this case all possible target nuclei can naturally be classified into n-odd and p-odd groups.

Following this classification the current experimental situation in the form of the exclusion curves for the spin-dependent WIMP-**proton** cross section is given in Fig. 5. The data are taken from experiments BRS, (NaI, 1992) [80,81], BPRS (CaF_2, 1993) [82], EDELWEISS (sapphire, 1996) [83], DAMA (NaI, 1996) [84], DAMA (CaF_2, 1999) [85,86], UKDMS (NaI, 1996) [87–90], ELEGANT (CaF_2, 1998) [91], ELEGANT (NaI, 1999) [92,93], Tokio (LiF, 1999, 2002) [94–98], SIMPLE (C_2ClF_5, 2001) [99], CRESST (Al_2O_3, 2002) [100], PICASSO (C_nF_m, 2002) [101], ANAIS (NaI, 2002) [102] and NAIAD (NaI, 2003) [103]. Although the DAMA/NaI-7 (2003) contours [2] are obtained on the basis of the positive and model-independent signature of the annual signal modulation (closed contour) as well as in the mixed coupling framework (open contour) [25] the contours for the WIMP-proton SD interaction (dominating in ^{127}I) are also presented in the figure (we will discuss the situation later).

The current experimental situation for the spin-dependent WIMP-**neutron** cross sections is given in Fig. 6. The data are taken from the first experiments with natural Ge (1988, 1991) [104,105], xenon (DAMA/Xe-0,2) [106–108], sodium iodide (NAIAD) [103], and from the HDMS experiment with a ^{73}Ge target [109]. Similar to Fig. 5 the DAMA/NaI-7 (2003) [2] contours for the WIMP-neutron SD interaction (subdominant in

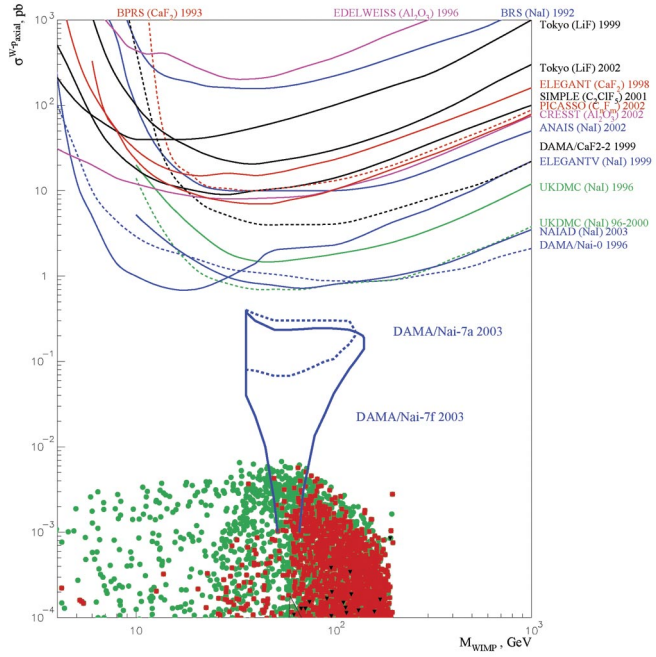

FIG. 5 (color online). Currently available exclusion curves for spin-dependent WIMP-proton cross sections ($\sigma^p_{\rm SD}$ as a function of WIMP-mass). The curves are obtained from [80–103]. DAMA/NaI-7a(f) contours for WIMP-proton SD interaction in ^{127}I are obtained on the basis of the positive and model-independent signature of annual signal modulation in the framework of a mixed scalar-spin coupling approach [2,25]. The scatter plots correspond to our calculations given in Figs. 2–4. The small trianglelike shaded area in the bottom is taken from [27]. Note that the *closed* DAMA contour is above the upper limit for $\sigma^p_{\rm SD} \approx 5 \times 10^{-2}$ pb.

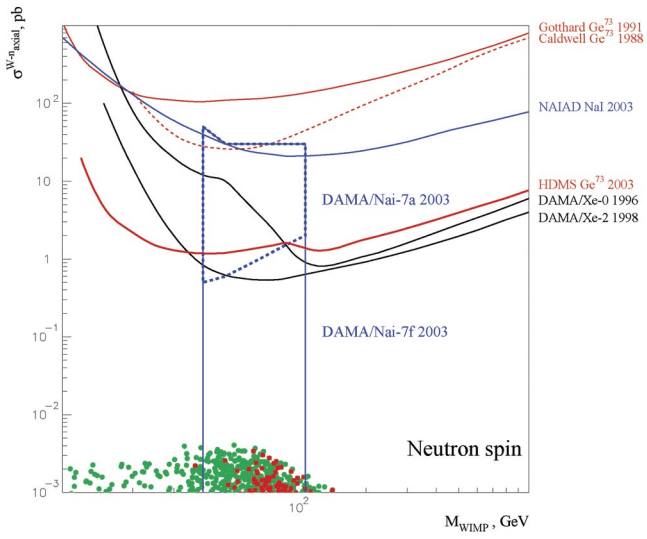

FIG. 6 (color online). Currently available exclusion curves for spin-dependent WIMP-neutron cross sections ($\sigma^n_{\rm SD}$ versus WIMP-mass). The curves are taken from [103–109]. DAMA/NaI-7a(f) contours for WIMP-neutron SD interaction (subdominating in ^{127}I) are obtained by us from the relevant figures of [2,25]. The scatter plots correspond to our calculations given in Figs. 2–4. Note that the NAIAD curve here corresponds to the subdominant for ^{127}I WIMP-neutron SD interaction. The curve was extracted from the nucleus ^{127}I (which has dominating WIMP-proton SD interaction) in the approach of [78]. It is much weaker in comparison with the relevant NAIAD curve for the WIMP-proton SD interaction in Fig. 5.

^{127}I) are placed in the figure. In the future one can also expect some exclusion curves for the SD cross section, for example, from the CDMS [110] and EDELWEISS [111] experiments with natural germanium bolometric detectors.

In Figs. 5 and 6 are also given scatter plots for SD proton and neutron cross sections which correspond to the results of our calculations shown in Figs. 2–4. From Figs. 5 and 6 one can, in general, conclude that an about 2 orders of magnitude improvement of the current DM experimental sensitivities (in the form of these exclusion curves) is needed to reach the SUSY predictions for the $\sigma^{p,n}_{\rm SD}$, provided the SUSY lightest neutralino is the best WIMP particle candidate.

Here we note that the calculated scatter plots for $\sigma^{p}_{\rm SD}$ (Fig. 5) are obtained without any assumption about $\sigma^{n}_{\rm SD} = 0$, but the experimental exclusion curves for $\sigma^{p}_{\rm SD}$ traditionally were extracted from the data under the full neglection of the spin-neutron contribution, i.e., under the assumption $\sigma^{n}_{\rm SD} = 0$. This one-spin-coupling dominance scheme (always used before a new approach was proposed in [78]) gave a bit too pessimistic exclusion curves, but allowed direct comparison of exclusion curves from different experiments. More stringent constraints on $\sigma^{p}_{\rm SD}$ one obtains following [1–3,78] assuming both $\sigma^{p}_{\rm SD} \neq 0$ and $\sigma^{n}_{\rm SD} \neq 0$ although usually the contribution of the neutron spin is very small ($\langle \mathbf{S}^A_n \rangle \ll \langle \mathbf{S}^A_p \rangle$). Therefore the direct comparison of old-fashioned exclusion curves with new ones is misleading *in general*. The same conclusion concerns [2,3] direct comparison of the SI exclusion curves (obtained without any SD contribution) with new SI exclusion curves (obtained with nonzero SD contribution) as well as with the results of the SUSY calculations (Fig. 1).

C. Mixed spin-scalar WIMP-nucleon interactions

Further more accurate calculations of spin nuclear structure [14,24,28–30,35,37,38,40–42] demonstrate that contrary to the simplified odd-group approach both $\langle \mathbf{S}^A_p \rangle$ and $\langle \mathbf{S}^A_n \rangle$ differ from zero, but nevertheless one of these spin quantities always dominates ($\langle \mathbf{S}^A_p \rangle \ll \langle \mathbf{S}^A_n \rangle$, or $\langle \mathbf{S}^A_n \rangle \ll \langle \mathbf{S}^A_p \rangle$). *If together* with the dominance like $\langle \mathbf{S}^A_{p(n)} \rangle \ll \langle \mathbf{S}^A_{n(p)} \rangle$ one would have the WIMP-proton and WIMP-neutron couplings of the same order of magnitude (*not* $a_{n(p)} \ll a_{p(n)}$), the situation could look like that in the odd-group model and one could safely (at the current level of accuracy) neglect subdominant spin contribution in the data analysis.

Nevertheless it was shown in [78] that in the general SUSY model one can meet right a case when $a_{n(p)} \ll a_{p(n)}$ and proton and neutron spin contributions are strongly mixed. To separately constrain the SD proton and neutron contributions at least two new approaches appeared in the literature [25,78]. As the authors of [78] claimed, their method has the advantage that the limits on individual WIMP-proton and WIMP-neutron SD cross sections for a given WIMP-mass can be combined to give a model-independent limit on the properties of WIMP scattering from both protons and neutrons in the target nucleus. The method relies on the assumption that the WIMP-nuclear SD cross section can be presented in the form $\sigma^A_{\rm SD}(0) = (\sqrt{\sigma^p_{\rm SD}|_A} \pm \sqrt{\sigma^n_{\rm SD}|_A})^2$, where $\sigma^p_{\rm SD}|_A$ and $\sigma^n_{\rm SD}|_A$ are auxiliary quantities, not directly connected with measurements. Furthermore, to extract, for example, a constraint on the subdominant WIMP-proton spin contribution one should assume the proton contribution dominance for a nucleus whose spin is almost completely determined by the neutron-odd group. From one side, this may look almost useless, especially because these subdominant constraints are always much weaker than the relevant constraints obtained directly with a proton-odd group target (one can compare, for example, the restrictive potential of the NAIAD exclusion curves in Figs. 5 and 6). From another side, the very large and very small ratios $\sigma_p/\sigma_n \sim a_p/a_n$ obtained in [78] correspond to neutralinos which are extremely pure gauginos. In this case Z-boson exchange in SD interactions is absent and only sfermions give contributions to SD cross sections. Obviously this is a very particular case which is also currently not in agreement with the experiments. Following an analogy between neutrinos and neutralinos one could assume that neutralino couplings with the neutron and the proton should not be very different [112] and one could expect preferably $|a_n|/|a_p| \approx O(1)$. We have checked the assumption in our effMSSM approach for large LSP masses in [55,56] and in this paper for relatively low LSP masses $m_\chi < 200$ GeV. Figure 7 shows that for the ratio of a_n to a_p we have the bounds

$$0.55 < |\frac{a_n}{a_p}| < 0.8. \tag{24}$$

The scatter plots in Fig. 7 as previously (see Fig. 2) were obtained with the relic neutralino density $0.0 < \Omega_\chi h^2_0 < 1.0$ (circles), with subdominant relic neutralino contribution $0.002 < \Omega_\chi h^2_0 < 0.1$ (squares) and with a WMAP-inspired relic neutralino density of $0.094 < \Omega_\chi h^2_0 < 0.129$ (triangles). Therefore in the model the couplings are almost the same and one can safely neglect, for example, the $\langle \mathbf{S}^A_p \rangle$-spin contribution in the analysis of the DM data for a nuclear target with $\langle \mathbf{S}^A_p \rangle \ll \langle \mathbf{S}^A_n \rangle$.

Furthermore, when one compares in the same figure an exclusion curve for SD WIMP-proton coupling obtained without subdominant SD WIMP-neutron contribution and without SI contribution (all curves in Fig. 5 except the one for NAIAD [103] and one for Tokyo-LiF [98]), with a curve from the approach of [78], when the subdominant

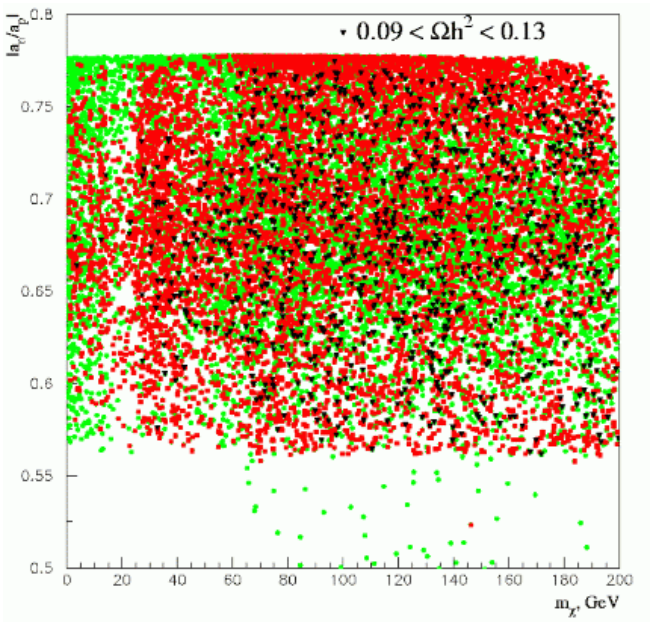

FIG. 7 (color online). The scatter plots (circles, squares, and triangles) give the ratio of the neutralino-neutron spin coupling a_n to the neutralino-proton spin coupling a_p in the effMSSM under the notations as in Figs. 2–4. The ratio is restricted to the range between 0.55 and 0.8.

contribution is included (the NAIAD and Tokyo-LiF curves in Fig. 5), one *"artificially"* improves the sensitivity of the *latter* curves (NAIAD or Tokyo-LiF) in comparison with the former ones. To be consistent and for reliable comparisons, one should coherently recalculate all previous curves in the new manner. This message is clearly also stressed in [2]. The same arguments are true for the last results of the SIMPLE experiment [113] and search for DM with NaF bolometers [114] where the SI contribution seems also completely ignored. Both above-mentioned results for fluorine will obviously be worse if (contrary to calculations of [41]) more reliable ^{19}F spin matrix elements (for example, from [30]) were used in their analysis. Although ^{19}F has the best properties for investigation of WIMP-nucleon spin-dependent interactions (see, for example [30]) it is not obvious that one should completely ignore spin-independent WIMP coupling with the fluorine. For example, in the relation $\sigma^A \sim \sigma^{A,p}_{\rm SD}[\sigma^A_{\rm SI}/\sigma^{A,p}_{\rm SD} + (1 + \sqrt{\sigma^{A,n}_{\rm SD}/\sigma^{A,p}_{\rm SD}})^2]$ which follows from (6)–(9), it is not *a priori* clear that $\sigma^A_{\rm SI}/\sigma^{A,p}_{\rm SD} \ll \sigma^{A,n}_{\rm SD}/\sigma^{A,p}_{\rm SD}$. At least for isotopes with atomic number $A > 50$ [15,22] the neglection of the SI contribution would be a larger mistake than the neglection of the subdominant SD WIMP-neutron contribution, when the SD WIMP-proton interaction dominates. Therefore we would like to note that the "old" odd-group-based approach in analyzing the SD data from experiments with heavy enough targets (for example, germanium) is still quite suitable. Especially when it is not obvious that (both) spin couplings dominate over the scalar one.

From measurements with ^{73}Ge one can extract, in principle, not only the dominant constraint for WIMP-nucleon coupling a_n (or $\sigma^n_{\rm SD}$) but also the constraint for the subdominant WIMP-proton coupling a_p (or $\sigma^p_{\rm SD}$) using the approach of [78]. Nevertheless, the latter constraint will be much weaker in comparison with the constraints from p-odd-group nuclear targets, like ^{19}F or I. This fact is illustrated by the NAIAD (NaI, 2003) curve in Fig. 6, which corresponds to the subdominant WIMP-neutron spin contribution extracted from the p-odd nucleus I.

Another approach of Bernabei *et al.* [25] looks in a more appropriate way for the mixed spin-scalar coupling data presentation, and is based on an introduction of the so-called effective SD nucleon cross section $\sigma^{pn}_{\rm SD}(0)$ (originally $\sigma_{\rm SD}$ in [2,25]) and coupling mixing angle θ (10) instead of $\sigma^p_{\rm SD}(0)$ and $\sigma^n_{\rm SD}(0)$. With these definitions the SD WIMP-proton and WIMP-neutron cross sections are given by relations (11).

In Fig. 8 the WIMP-nucleon spin and scalar mixed couplings allowed by the annual modulation signature from the 100 kg DAMA/NaI experiment are shown inside the shaded regions. The regions from [2,25] in the ($\xi\sigma_{\rm SI}$, $\xi\sigma_{\rm SD}$) space for 40 GeV $< m_{\rm WIMP} <$ 110 GeV cover spin-scalar mixing coupling for the proton ($\theta = 0$ case of [2,25], upper panel) and spin-scalar mixing coupling for the neutron ($\theta = \pi/2$, lower panel). From nuclear physics one has for the proton spin dominated ^{23}Na and ^{127}I, $\frac{\langle \mathbf{S}_n \rangle}{\langle \mathbf{S}_p \rangle} < 0.1$ and $\frac{\langle \mathbf{S}_n \rangle}{\langle \mathbf{S}_p \rangle} < 0.02 \div 0.23$, respectively. For the $\theta = 0$ due to the p-oddness of the I target, the DAMA WIMP-proton spin constraint is the most severe one (see Fig. 5).

In the lower panel of Fig. 8 we present the exclusion curve (dashed line) for the WIMP-proton spin coupling from the proton-odd isotope ^{129}Xe obtained under the mixed coupling assumptions [25] from the DAMA-LiXe (1998) experiment [108,115,116]. For the DAMA-NaI detector the $\theta = \pi/2$ means no $\langle \mathbf{S}_p \rangle$ contribution at all. Therefore, in this case DAMA gives the subdominant $\langle \mathbf{S}_n \rangle$ contribution only, which could be compared further with the dominant $\langle \mathbf{S}_n \rangle$ contribution in ^{73}Ge.

The scatter plots in Fig. 8 give $\sigma^p_{\rm SI}$ as a function of $\sigma^p_{\rm SD}$ (upper panel) and $\sigma^n_{\rm SD}$ (lower panel) calculated in this work in the effMSSM with parameters from (23) under the same constraints on the relic neutralino density as in Figs. 2–4. Filled circles correspond to relic neutralino density $0.0 < \Omega_\chi h^2_0 < 1.0$, squares correspond to subdominant relic neutralino contribution $0.002 < \Omega_\chi h^2_0 < 0.1$ and triangles correspond to WMAP density constraint $0.094 < \Omega_\chi h^2_0 < 0.129$.

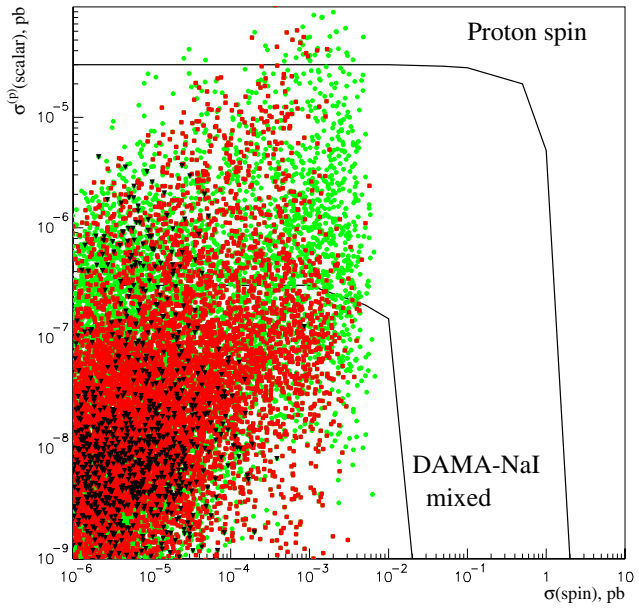

FIG. 8 (color online). The DAMA-NaI region from the WIMP annual modulation signature in the $(\xi\sigma_{\rm SI}, \xi\sigma_{\rm SD})$ space for $40 < m_{\rm WIMP} < 110$ GeV [2,25]. Upper panel corresponds to dominating (in ^{127}I) SD proton coupling only ($\theta = 0$) and lower panel corresponds to subdominating SD neutron coupling only ($\theta = \pi/2$). The scatter plots give correlations between $\sigma^p_{\rm SI}$ and $\sigma_{\rm SD}$ in the effMSSM ($\xi = 1$ is assumed) for $m_\chi < 200$ GeV under the same notations as in Figs. 2–4. In the right panel the DAMA liquid xenon exclusion curve from [25] is given (dashed line).

The constraints on the SUSY parameter space in the mixed coupling framework in Fig. 8 are, in general, much stronger in comparison with the traditional approach based on the one-coupling dominance (Figs. 1, 5 and 6).

It follows from Fig. 8, that when the LSP is the sub dominant DM particle (squares in the figure) SD WIMP-proton and WIMP-neutron cross sections at a level of $3 \div 5 \times 10^{-3}$ pb are allowed, but the WMAP relic density constraint (triangles) together with the DAMA restrictions leaves only $\sigma^{p,n}_{\rm SD} < 3 \times 10^{-5}$ pb without any visible reduction of allowed values for $\sigma^p_{\rm SI}$. In general, according to the DAMA restrictions, small SI cross sections are completely excluded, only $\sigma^p_{\rm SI} > 3 \div 5 \times 10^{-7}$ pb are allowed. Concerning the SD cross section the situation is not clear, because for the allowed values of the SI contribution, the SD DAMA sensitivity did not yet reach the calculated upper bound for the SD LSP-proton cross section of 5×10^{-2} pb.

D. The mixed couplings case for the high-spin ^{73}Ge

Comparing the number of exclusion curves in Figs. 5 and 6 one can see that there are many measurements with p-odd nuclei and there is a lack of data for n-odd nuclei, i.e., for $\sigma^n_{\rm SD}$. Therefore measurements with n-odd nuclei are needed. From our point of view this lack of $\sigma^n_{\rm SD}$ measurements can be filled with new data expected from the HDMS experiment with the high-spin isotope ^{73}Ge [10]. This isotope looks with a good accuracy like an almost pure n-odd group nucleus with $\langle \mathbf{S}_n \rangle \gg \langle \mathbf{S}_p \rangle$ (Table I). The variation of the $\langle \mathbf{S}_p \rangle$ and $\langle \mathbf{S}_n \rangle$ in the table reflects the level of inaccuracy and complexity of the current nuclear structure calculations.

In the mixed spin-scalar coupling case for ^{73}Ge the direct detection rate integrated over recoil energy (21) from threshold energy, ϵ, until maximal energy ε can be presented in the form

$$
\begin{aligned}
R(\epsilon, \varepsilon) &= \alpha(\epsilon, \varepsilon, m_\chi)\sigma^p_{\rm SI} + \beta(\epsilon, \varepsilon, m_\chi)\sigma^n_{\rm SD};\\
\alpha(\epsilon, \varepsilon, m_\chi) &= N_T \frac{\rho_\chi M_A}{2 m_\chi \mu_p^2} A^2 A_{\rm SI}(\epsilon, \varepsilon),\\
\beta(\epsilon, \varepsilon, m_\chi) &= N_T \frac{\rho_\chi M_A}{2 m_\chi \mu_p^2} \frac{4}{3} \frac{J+1}{J} \langle \mathbf{S}^A_n \rangle^2 A_{\rm SD}(\epsilon, \varepsilon).
\end{aligned}
\tag{25}
$$

The convolutions of nuclear form-factors with the WIMP velocity distributions, $A_{\rm SI,SD}(\epsilon, \varepsilon)$, are defined by expressions (22). We neglect for ^{73}Ge the subdominant contribution from WIMP-proton spin coupling proportional to $\langle \mathbf{S}^A_p \rangle$. We consider only a simple spherically symmetric isothermal WIMP velocity distribution [33,118] and do not go into details of any possible and in principle important uncertainties (and/or modulation effects) of the Galactic halo WIMP distribution [119–125]. For simplicity we use the Gaussian scalar

TABLE I. All available calculations in different nuclear models for the zero-momentum spin structure (and predicted magnetic moments μ) of the ^{73}Ge nucleus. The experimental value of the magnetic moment given in the brackets is used as input in the calculations.

^{73}Ge ($G_{9/2}$)	$\langle \mathbf{S}_p \rangle$	$\langle \mathbf{S}_n \rangle$	μ (in μ_N)
ISPSM, Ellis-Flores [34,117]	0	0.5	-1.913
OGM, Engel-Vogel [43]	0	0.23	$(-0.879)_{\rm exp}$
IBFM, Iachello *et al.* [24,42]	-0.009	0.469	-1.785
IBFM (quenched), Iachello *et al.* [24,42]	-0.005	0.245	$(-0.879)_{\rm exp}$
TFFS, Nikolaev-Klapdor-Kleingrothaus, [44]	0	0.34	
SM (small), Ressell *et al.* [24]	0.005	0.496	-1.468
SM (large), Ressell *et al.* [24]	0.011	0.468	-1.239
SM (large, quenched), Ressell *et al.* [24]	0.009	0.372	$(-0.879)_{\rm exp}$
Hybrid SM, Dimitrov *et al.* [37]	0.030	0.378	-0.920

and spin nuclear form-factors from [117,126]. For the relic neutralino mass density and for the escape neutralino velocity we use the values 0.3 GeV/ cm^3 and 600 km/s, respectively. With formulas (25), we perform below a simple estimation of prospects for DM search and SUSY constraints with the high-spin ^{73}Ge detector HDMS assuming mixing of WIMP-neutron spin and WIMP-nucleon scalar couplings together with available results from the DAMA-NaI and LiXe experiments [1–3,108,115,116].

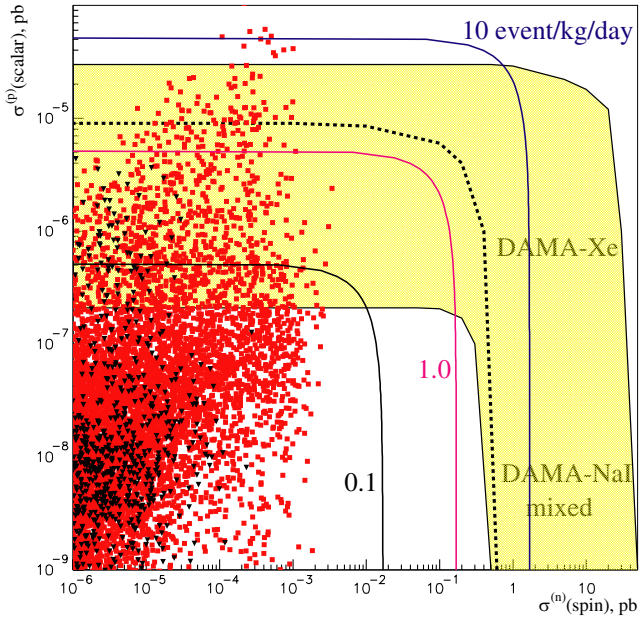

FIG. 9 (color online). The solid lines (marked with numbers of $R(15, 50)$ in events/kg/day) show the sensitivities of the HDMS setup with ^{73}Ge in the framework of mixed SD WIMP-neutron and SI WIMP-nucleon couplings. The DAMA-NaI region for subdominant SD WIMP-neutron coupling ($\theta = \pi/2$) is from Fig. 8. Scatter plots give correlations between $\sigma^p_{\rm SI}$ and $\sigma^n_{\rm SD}$ in the effMSSM for $m_\chi < 200$ GeV. The squares correspond to subdominant relic neutralino contribution $0.002 < \Omega_\chi h_0^2 < 0.1$ and triangles correspond to WMAP relic neutralino density $0.094 < \Omega_\chi h_0^2 < 0.129$. The dashed line from [25] shows the DAMA-LiXe (1998) exclusion curve for $m_{\rm WIMP} = 50$ GeV.

The Heidelberg Dark Matter Search (HDMS) experiment uses a special configuration of two Ge detectors to efficiently reduce the background [10,127]. From the first preliminary results of the HDMS experiment with inner HPGe crystal of enriched ^{73}Ge [10,109] we can estimate the current background event rate $R(\epsilon, \varepsilon)$ integrated here from the "threshold" energy $\epsilon =$ 15 keV to "maximal" energy $\varepsilon = 50$ keV. We obtain $R(15, 50) \approx 10$ events/kg/day. A substantial improvement of the background (up to an order of magnitude) is further expected for the setup in the Gran Sasso Underground Laboratory. In Fig. 9 solid lines for the integrated rate $R(15, 50)$ marked with numbers 10, 1.0 and 0.1 (in events/kg/day) present for $m_{\rm WIMP} = 70$ GeV our exclusion curves expected from the HDMS setup with ^{73}Ge in the framework of mixed SD WIMP-neutron and SI WIMP-nucleon couplings. Unfortunately the current background index for HDMS is not yet optimized, and the relevant exclusion curve (marked with 10 events/kg/day) has almost the same strength to reduce $\sigma^n_{\rm SD}$ as the dashed curve from the DAMA experiment with liquid Xe [25] obtained for $m_{\rm WIMP} = 50$ GeV (better sensitivity is expected with HDMS for $m_{\rm WIMP} < 40$ GeV). However, both experiments lead already to some sharper restriction for $\sigma^n_{\rm SD}$ then obtained by DAMA (see Fig. 9). One order of magnitude improvement of the HDMS sensitivity (curve marked with 1.0) will supply us with the best exclusion curve for SD WIMP-neutron coupling, but this sensitivity is not yet enough to reach the calculated upper bound for $\sigma^n_{\rm SD}$. This sensitivity also could reduce the upper bound for SI WIMP-proton coupling $\sigma^p_{\rm SI}$ to a level of 10^{-5} pb. Nevertheless, only an *additional* about 1 order of magnitude HDMS sensitivity improvement is needed to obtain decisive constraints on $\sigma^p_{\rm SI}$ as well as on $\sigma^n_{\rm SD}$. In this case only

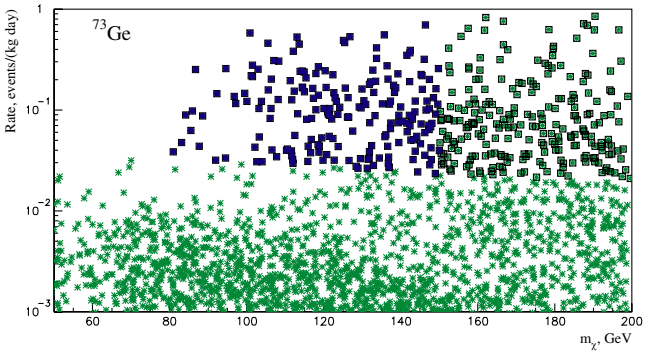

FIG. 10 (color online). Event rate for direct neutralino detection in a ^{73}Ge detector as function of the LSP neutralino mass. Crosses present our calculations with relic density constraint $0.1 < \Omega_\chi h_0^2 < 0.3$ only. Open boxes correspond to implementation of the SI cross section limit 1×10^{-7} pb $< \sigma^p_{\rm SI}(0) < 3 \times 10^{-5}$ pb only, and closed boxes show results with the additional WIMP-mass constraint $40 < m_{\rm WIMP} < 150$ GeV (see (26)).

quite narrow bounds for these cross sections will be allowed (below the curve marked by 0.1 and above the lower bound of DAMA-NaI mixed region). In practice it seems, that only the DAMA and the HDMS constraints *together* could restrict the SD WIMP-neutron coupling sufficiently.

E. Some other consequences of the DAMA results

It follows from Figs. 1, 5, 6 and 8 that the main results of the DAMA experiment one could summarize in the limitations of the WIMP-mass, and the restrictions on the cross section of the *scalar* WIMP-proton interaction. Quite approximately (having in mind all possible uncertainties of [2,3]) one can write them in the form:

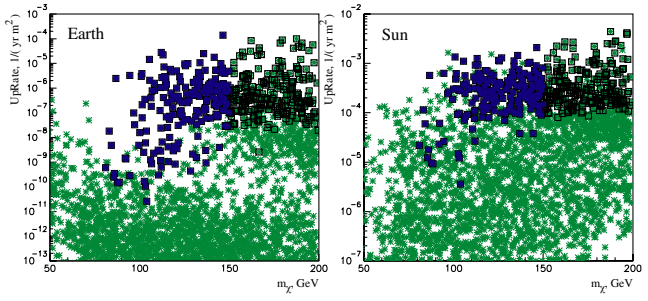

FIG. 11 (color online). Indirect detection rate for upgoing muons from DM particles (neutralinos) annihilation in (a) the Earth and (b) the Sun as function of the LSP neutralino mass. Crosses present our calculations with relic density constraint $0.1 < \Omega_\chi h_0^2 < 0.3$ only. Open boxes correspond to implementation of the SI cross section limits of (26) only and closed boxes depict results with both limitations of (26).

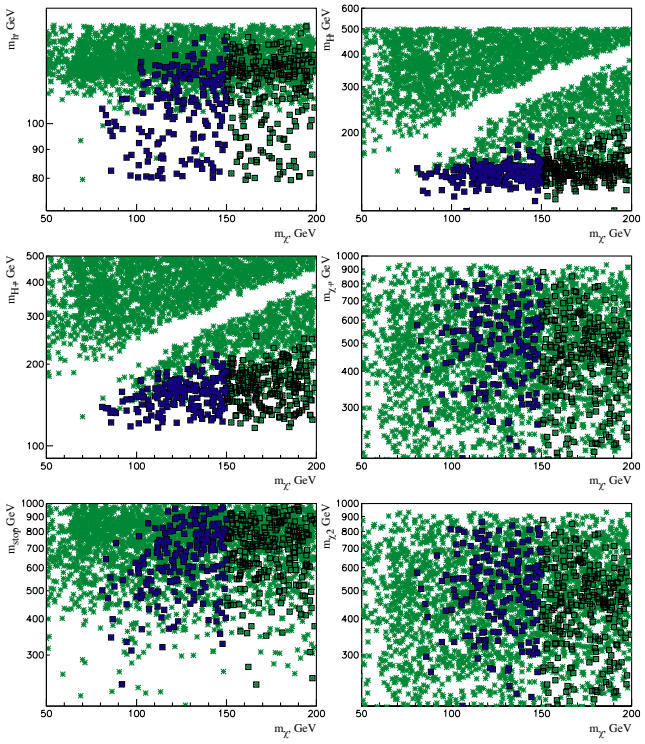

FIG. 12 (color online). Masses in GeV of light ($m_{\rm h}$), heavy ($m_{\rm H}$), and charged Higgs bosons ($m_{\rm H^+}$), as well as masses of chargino (m_{χ^+}), stop ($m_{\rm stop}$), and second neutralino (m_{χ^2}), versus the mass (m_χ) of the LSP neutralino under the same DAMA-inspired restrictions as in Figs. 10 and 11.

$$40 \text{ GeV} < m_{\rm WIMP} < 150 \text{ GeV}, \qquad 1 \times 10^{-7} \text{ pb} < \sigma^p_{\rm SI(0)} < 3 \times 10^{-5} \text{ pb}. \tag{26}$$

The limitations of (26) should have some consequence for observables. Taking them into account we have obtained the reduction of our scatter plots for the total expected event rate of direct WIMP detection in a ^{73}Ge detector (Fig. 10) and the indirect detection rate for upgoing muons from dark matter particles annihilation in the Earth and the Sun (Fig. 11). The calculations of indirect detection rates follow the description given in [15,128]. There is also a reduction of allowed masses of some SUSY particles (Fig. 12). In total from these figures one can see that the DAMA evidence favors the light Higgs sector of the MSSM, relatively high event rate in Ge detectors, as well as relatively high upgoing muon fluxes from the Earth and from the Sun for indirect detection of the relic neutralino. It is also almost insensitive to the sfermion and neutralino-chargino particle masses. As noted before in [46,128] the relatively light Higgs masses (smaller than 200 GeV) are very interesting from the point of accelerator SUSY searches.

IV. CONCLUSION

In the effective low-energy MSSM (effMSSM) for zero-momentum transfer we calculated the LSP-proton(neutron) spin and scalar cross sections in the low LSP mass regime, which follows from the DAMA dark matter evidence. We compared the calculated cross sections with experimental exclusion curves and demonstrated that about 2 orders of magnitude improvement of the current DM experiment sensitivities is needed to reach the SUSY predictions for the $\sigma^{p,n}_{\rm SD}$.

We noted an in principle possible incorrectness in the direct comparison of exclusion curves for WIMP-proton(neutron) spin-dependent cross section obtained with and without nonzero WIMP-neutron(proton) spin-dependent contribution. On the other side, nuclear spin structure calculations show that usually one, WIMP-proton $\langle \mathbf{S}^A_p \rangle$, or WIMP-neutron $\langle \mathbf{S}^A_n \rangle$, nuclear spin dominates and in the effMSSM we have the WIMP-proton and WIMP-neutron effective couplings a_n and a_p of the same order of magnitude (Fig. 7). Therefore at the current level of accuracy it looks reasonable to safely neglect subdominant WIMP-nucleon contributions analyzing the data from spin-nonzero targets. Furthermore the above-mentioned incorrectness concerns also the direct comparison of spin-dependent exclusion curves obtained with and without nonzero spin-independent contributions [2,3]. To be consistent, for this comparison one has to use a mixed spin-scalar coupling approach (Figs. 8 and 9),as for the first time proposed by the DAMA collaboration [1–3]. We applied such spin-scalar coupling approach to estimate future prospects of the HDMS experiment with the neutron-odd group high-spin isotope ^{73}Ge. Although the odd-neutron nuclei ^{73}Ge, ^{129}Xe already with the present accuracy lead to some sharper restrictions for $\sigma^n_{\rm SD}$ then obtained by DAMA, we found that the current accuracy of measurements with ^{73}Ge (as well as with ^{129}Xe and NaI) did not yet reach a level which allows us to obtain new decisive constraints on the SUSY parameters. Future about 2 orders of magnitude improvement of the background index in the HDMS experiment [10] can in principle supply us with new constraints for the SUSY models.

Finally we noticed that the DAMA evidence favors the light Higgs sector in the effMSSM (which could be reached at LHC), a high event rate in a ^{73}Ge detector and relatively high upgoing muon fluxes from relic neutralino annihilations in the Earth and the Sun.

ACKNOWLEDGMENTS

V. B. thanks the Max-Planck Institut für Kernphysik for the hospitality and RFBR (Grant No. 02-02-04009) for support.

[1] R. Bernabei *et al.*, Phys. Lett. B **480**, 23 (2000).
[2] R. Bernabei *et al.*, Rivista del Nuovo Cimento **26**, 1 (2003).
[3] R. Bernabei *et al.*, astro-ph/0311046.
[4] C. J. Copi and L. M. Krauss, Phys. Rev. D **67**, 103507 (2003).
[5] A. Kurylov and M. Kamionkowski, Phys. Rev. D **69**, 063503 (2004).
[6] D. Tucker-Smith and N. Weiner, hep-ph/0402065.
[7] G. Gelmini and P. Gondolo, hep-ph/0405278.
[8] H.V. Klapdor-Kleingrothaus, O. Chkvorez, I.V. Krivosheina, H. Strecker, and C. Tomei, Nucl. Instrum. Methods Phys. Res., Sect. A **511**, 341 (2003).
[9] C. Tomei, A. Dietz, I. Krivosheina, and H.V. Klapdor-Kleingrothaus, Nucl. Instrum. Methods Phys. Res., Sect. A **508**, 343 (2003).
[10] H.V. Klapdor-Kleingrothaus *et al.*, Astropart. Phys. **18**, 525 (2003).
[11] V. A. Bednyakov, H.V. Klapdor-Kleingrothaus, and S. G. Kovalenko, Phys. Lett. B **329**, 5 (1994).
[12] V. A. Bednyakov and H.V. Klapdor-Kleingrothaus, Phys. Rev. D **63**, 095005 (2001).
[13] V. A. Bednyakov, Phys. At. Nucl. **66**, 490 (2003).
[14] J. Engel, Phys. Lett. B **264**, 114 (1991).
[15] G. Jungman, M. Kamionkowski, and K. Griest, Phys. Rep. **267**, 195 (1996).
[16] J. D. Lewin and P. F. Smith, Astropart. Phys. **6**, 87 (1996).
[17] P. F. Smith and J. D. Lewin, Phys. Rep. **187**, 203 (1990).
[18] V. A. Bednyakov and H.V. Klapdor-Kleingrothaus, Phys. At. Nucl. **62**, 966 (1999).
[19] V. A. Bednyakov, S. G. Kovalenko, and H.V. Klapdor-Kleingrothaus, Phys. At. Nucl. **59**, 1718 (1996).
[20] V. A. Bednyakov, H.V. Klapdor-Kleingrothaus, and S. G. Kovalenko, Phys. Rev. D **55**, 503 (1997).
[21] V. A. Bednyakov, S. G. Kovalenko, H.V. Klapdor-Kleingrothaus, and Y. Ramachers, Z. Phys. A: Hadrons Nucl. **357**, 339 (1997).
[22] V. A. Bednyakov, H.V. Klapdor-Kleingrothaus, and S. Kovalenko, Phys. Rev. D **50**, 7128 (1994).
[23] J. Engel, S. Pittel, and P. Vogel, Int. J. Mod. Phys. E **1**, 1 (1992).
[24] M. T. Ressell *et al.*, Phys. Rev. D **48**, 5519 (1993).
[25] R. Bernabei *et al.*, Phys. Lett. B **509**, 197 (2001).
[26] G. K. Mallot, Int. J. Mod. Phys. A **15S1**, 521 (2000).
[27] J. R. Ellis, A. Ferstl, and K. A. Olive, Phys. Lett. B **481**, 304 (2000).
[28] J. Engel, M. T. Ressell, I. S. Towner, and W. E. Ormand, Phys. Rev. C **52**, 2216 (1995).

[29] M. T. Ressell and D. J. Dean, Phys. Rev. C **56**, 535 (1997).
[30] P. C. Divari, T. S. Kosmas, J. D. Vergados, and L. D. Skouras, Phys. Rev. C **61**, 054612 (2000).
[31] K. Griest, Phys. Rev. D **38**, 2357 (1988).
[32] M. W. Goodman and E. Witten, Phys. Rev. D **31**, 3059 (1985).
[33] A. K. Drukier, K. Freese, and D. N. Spergel, Phys. Rev. D **33**, 3495 (1986).
[34] J. R. Ellis and R. A. Flores, Nucl. Phys. B **307**, 883 (1988).
[35] J. D. Vergados, J. Phys. G **22**, 253 (1996).
[36] J. D. Vergados, Phys. At. Nucl. **66**, 481 (2003).
[37] V. Dimitrov, J. Engel, and S. Pittel, Phys. Rev. D **51**, 291 (1995).
[38] J. Engel, S. Pittel, E. Ormand, and P. Vogel, Phys. Lett. B **275**, 119 (1992).
[39] M. A. Nikolaev and H. V. Klapdor-Kleingrothaus, Z. Phys. A: Hadrons Nucl. **345**, 183 (1993).
[40] T. S. Kosmas and J. D. Vergados, Phys. Rev. D **55**, 1752 (1997).
[41] A. F. Pacheco and D. Strottman, Phys. Rev. D **40**, 2131 (1989).
[42] F. Iachello, L. M. Krauss, and G. Maino, Phys. Lett. B **254**, 220 (1991).
[43] J. Engel and P. Vogel, Phys. Rev. D **40**, 3132 (1989).
[44] M. A. Nikolaev and H. V. Klapdor-Kleingrothaus, Z. Phys. A: Hadrons Nucl. **345**, 373 (1993).
[45] R. Bernabei *et al.*, in Proceedings of 10th International Workshop on Neutrino Telescopes, Venice, Italy, 2003 Vol. 2, p. 403, astro-ph/0305542.
[46] V. A. Bednyakov and H. V. Klapdor-Kleingrothaus, Phys. Rev. D **62**, 043524 (2000).
[47] V. Mandic, A. Pierce, P. Gondolo, and H. Murayama, hep-ph/0008022.
[48] L. Bergstrom and P. Gondolo, Astropart. Phys. **5**, 263 (1996); also in *Proceedings of 4th International Symposium on Sources and Detection of Dark Matter in the Universe (DM 2000), Marina del Rey, California, 2000*, edited by D. Cline (Springer, New York, 2001) p. 177.
[49] P. Gondolo, in *Sources and Detection of Dark Matter and Dark Energy in the Universe, Marina del Rey, 2000* (Springer-Verlag, Berlin, 2001), p. 177, hep-ph/0005171.
[50] V. A. Bednyakov and H. V. Klapdor-Kleingrothaus, Phys. Rev. D **59**, 023514 (1999).
[51] L. Bergstrom, Rep. Prog. Phys. **63**, 793 (2000).
[52] A. Bottino, F. Donato, N. Fornengo, and S. Scopel, Phys. Rev. D **63**, 125003 (2001).
[53] J. R. Ellis, K. A. Olive, Y. Santoso, and V. C. Spanos, Phys. Rev. D **69**, 015005 (2004).
[54] J. R. Ellis, A. Ferstl, K. A. Olive, and Y. Santoso, Phys. Rev. D **67**, 123502 (2003).
[55] V. A. Bednyakov, hep-ph/0310041.
[56] V. A. Bednyakov, H. V. Klapdor-Kleingrothaus, and V. Gronewold, Phys. Rev. D **66**, 115005 (2002).
[57] V. A. Bednyakov, H. V. Klapdor-Kleingrothaus, and E. Zaiti, Phys. Rev. D **66**, 015010 (2002).
[58] V. A. Bednyakov, in *Beyond the Desert, Oulu, 2002* (IOP, Bristol, 2003), p. 451 (hep-ph/0208172).
[59] M. Drees *et al.*, Phys. Rev. D **63**, 035008 (2001).
[60] R. Arnowitt, B. Dutta, and Y. Santoso, hep-ph/0008336.
[61] A. Corsetti and P. Nath, in Results and Perspectives in Particle Physics, La Thuile, 2000, p. 583, hep-ph/0005234.
[62] K. Hagiwara *et al.*, Phys. Rev. D **66**, 010001 (2002).
[63] M. S. Alam *et al.*, Phys. Rev. Lett. **74**, 2885 (1995).
[64] K. Abe *et al.*, in *20th International Symposium on Lepton and Photon Interactions at High Energies (LP 01), Rome, 2001* (World Scientific, Singapore, 2003).
[65] S. Bertolini, F. Borzumati, A. Masiero, and G. Ridolfi, Nucl. Phys. B **353**, 591 (1991).
[66] R. Barbieri and G. F. Giudice, Phys. Lett. B **309**, 86 (1993).
[67] A. J. Buras, M. Misiak, M. Munz, and S. Pokorski, Nucl. Phys. B **424**, 374 (1994).
[68] A. Ali and C. Greub, Z. Phys. C **60**, 433 (1993).
[69] P. Gondolo, J. Edsjo, L. Bergstrom, P. Ullio, and E. A. Baltz, in *The Identification of Dark Matter, York, 2000* (World Scientific, Singapore, 2001), p. 318 (astro-ph/0012234).
[70] D. N. Spergel *et al.*, Astrophys. J. Suppl. Ser. **148**, 175 (2003).
[71] C. L. Bennett *et al.*, Astrophys. J. Suppl. Ser. **148**, 1 (2003).
[72] A. Bottino, F. Donato, N. Fornengo, and S. Scopel, Phys. Rev. D **69**, 037302 (2004).
[73] J. L. Feng, K. T. Matchev, and F. Wilczek, Phys. Lett. B **482**, 388 (2000).
[74] E. Accomando, R. Arnowitt, B. Dutta, and Y. Santoso, Nucl. Phys. B **585**, 124 (2000).
[75] E. Gabrielli, S. Khalil, C. Munoz, and E. Torrente-Lujan, Phys. Rev. D **63**, 025008 (2001).
[76] H. Baer and M. Brhlik, Phys. Rev. D **57**, 567 (1998).
[77] A. B. Lahanas, D. V. Nanopoulos, and V. C. Spanos, Mod. Phys. Lett. A **16**, 1229 (2001).
[78] D. R. Tovey, R. J. Gaitskell, P. Gondolo, Y. Ramachers, and L. Roszkowski, Phys. Lett. B **488**, 17 (2000).
[79] P. Ullio, M. Kamionkowski, and P. Vogel, J. High Energy Phys. 07 (2001) 044.
[80] C. Bacci *et al.*, Nucl. Phys. B, Proc. Suppl. **35**, 159 (1994).
[81] C. Bacci *et al.*, Phys. Lett. B **293**, 460 (1992).
[82] C. Bacci *et al.*, Astropart. Phys. **2**, 117 (1994).
[83] A. de Bellefon *et al.*, Astropart. Phys. **6**, 35 (1996).
[84] R. Bernabei *et al.*, Phys. Lett. B **389**, 757 (1996).
[85] R. Bernabei *et al.*, Astropart. Phys. **7**, 73 (1997).
[86] P. Belli *et al.*, Nucl. Phys. B **563**, 97 (1999).
[87] M. L. Sarsa *et al.*, Phys. Lett. B **386**, 458 (1996).
[88] P. F. Smith *et al.*, Phys. Lett. B **379**, 299 (1996).
[89] T. J. Sumner *et al.*, Nucl. Phys. B, Proc. Suppl. **70**, 74 (1999).
[90] N. J. C. Spooner *et al.*, Phys. Lett. B **473**, 330 (2000).
[91] I. Ogawa *et al.*, Nucl. Phys. A **663**, 869 (2000).
[92] K. Fushimi *et al.*, Astropart. Phys. **12**, 185 (1999).
[93] S. Yoshida *et al.*, Nucl. Phys. B, Proc. Suppl. **87**, 58 (2000).
[94] W. Ootani *et al.*, Astropart. Phys. **9**, 325 (1998).
[95] M. Minowa, Phys. At. Nucl. **61**, 1117 (1998).
[96] W. Ootani *et al.*, Phys. Lett. B **461**, 371 (1999).

[97] W. Ootani *et al.*, Nucl. Instrum. Methods Phys. Res., Sect. A **436**, 233 (1999).
[98] K. Miuchi *et al.*, Astropart. Phys. **19**, 135 (2003).
[99] J. I. Collar *et al.*, in The Identification of Dark Matter, York, 2000 (Ref. [69]), p. 397 (astro-ph/0101176).
[100] G. Angloher *et al.*, Astropart. Phys. **18**, 43 (2002).
[101] N. Boukhira *et al.*, Nucl. Phys. B, Proc. Suppl. **110**, 103 (2002).
[102] S. Cebrian *et al.*, Nucl. Phys. B, Proc. Suppl. **114**, 111 (2003).
[103] B. Ahmed *et al.*, Astropart. Phys. **19**, 691 (2003).
[104] D. O. Caldwell *et al.*, Phys. Rev. Lett. **61**, 510 (1988).
[105] D. Reusser *et al.*, Phys. Lett. B **255**, 143 (1991).
[106] P. Belli *et al.*, Nuovo Cimento Soc. Ital. Fis., C **19**, 537 (1996).
[107] P. Belli *et al.*, Nucl. Phys. B, Proc. Suppl. **48**, 62 (1996).
[108] R. Bernabei *et al.*, Phys. Lett. B **436**, 379 (1998).
[109] H.V. Klapdor-Kleingrothaus *et al.* (to be published).
[110] D. S. Akerib *et al.*, Phys. Rev. D **68**, 082002 (2003).
[111] A. Benoit *et al.*, Phys. Lett. B **545**, 43 (2002).
[112] J. D. Vergados (private communication).
[113] F. Giuliani and T. Girard, Phys. Lett. B **588**, 151 (2004).
[114] A. Takeda *et al.*, Phys. Lett. B **572**, 145 (2003).
[115] R. Bernabei *et al.*, Nucl. Phys. B, Proc. Suppl. **110**, 88 (2002).
[116] R. Bernabei *et al.*, Nucl. Instrum. Methods Phys. Res., Sect. A **482**, 728 (2002).
[117] J. R. Ellis and R. A. Flores, Phys. Lett. B **263**, 259 (1991).
[118] K. Freese, J. A. Frieman, and A. Gould, Phys. Rev. D **37**, 3388 (1988).
[119] A. Kinkhabwala and M. Kamionkowski, Phys. Rev. Lett. **82**, 4172 (1999).
[120] F. Donato, N. Fornengo, and S. Scopel, Astropart. Phys. **9**, 247 (1998).
[121] N.W. Evans, C. M. Carollo, and P.T. de Zeeuw, Mon. Not. R. Astron. Soc. **318**, 1131 (2000).
[122] A. M. Green, Phys. Rev. D **63**, 043005 (2001).
[123] C. J. Copi and L. M. Krauss, Phys. Rev. D **63**, 043507 (2001).
[124] P. Ullio and M. Kamionkowski, J. High Energy Phys. 03 (2001) 049.
[125] J. D. Vergados, Part. Nucl. Lett. **106**, 74 (2001).
[126] J. R. Ellis and R. A. Flores, Phys. Lett. B **300**, 175 (1993).
[127] H.V. Klapdor-Kleingrothaus *et al.*, in The Identification of Dark Matter, York, 2000 (World Scientific, Singapore, 2001), p. 415.
[128] V. A. Bednyakov, H.V. Klapdor-Kleingrothaus, and H. Tu, Phys. Rev. D **64**, 075004 (2001).